

The effects of CuO doping on structural, electrical and optical properties of CdO thin films deposited by pulsed laser deposition technique

S. M. A. Al-Dujayli*, N. A. Ali

Department of Physics, Collage of Science, University of Baghdad, Baghdad, Iraq

Thin films of $(\text{CdO})_x (\text{CuO})_{1-x}$ (where $x = 0.0, 0.2, 0.3, 0.4$ and 0.5) were prepared by the pulsed laser deposition. The CuO addition caused an increase in diffraction peaks intensity at (111) and a decrease in diffraction peaks intensity at (200). As CuO content increases, the band gap increases to a maximum of 3.51 eV, maximum resistivity of $8.251 \times 10^4 \Omega \cdot \text{cm}$ with mobility of $199.5 \text{ cm}^2/\text{V}\cdot\text{s}$, when $x = 0.5$. The results show that the conductivity is n-type when x value was changed in the range (0 to 0.4) but further addition of CuO converted the samples to p-type.

(Received April 19, 2022; Accepted August 1, 2022)

Keywords: Cadmium oxide, XRD, Optical properties, Pulse laser deposition

1. Introduction

Some metal oxides like Zinc, Indium, Cadmium and Tin show different behaviors as metals or insulators depending on their optical and electrical properties [1]. Transparent conductive oxide (TCO) thin films have many unique properties such as high optical transmittance and low resistivity. Because of this, they have been employed in many applications [2]. CdO is one example of transparent conductive oxide. They exhibit excellent properties like high electric conductivity and moderate refractive index. In addition, they are selectively transmitting layers i.e. they have high transmittance in the visible region and reflective to infrared radiation [3]. Studies have shown that CdO possess band gap in the range 2.2 to 2.8 eV, resistivity value of $(10^{-2} - 10^{-4} \Omega \cdot \text{cm})$ and showed negative conductance [4, 5]. These significant properties make it suitable for many applications in the optoelectronics field such as photovoltaic solar cells, phototransistors, liquid crystal displays, gas sensors, and other optoelectronic devices [6-8]. It is noteworthy that the properties of CdO depend on its synthesis method and preparing conditions [9]. Many techniques are employed to prepare CdO thin films such as pulsed laser deposition, thermal evaporation, spin coating, chemical bath deposition, spray pyrolysis, sol-gel method and sputtering [10-13]. The pulsed laser technique was used to prepared thin films from different types of materials [14].

PLD is a thin film deposition technique, where flashes of laser are used to generate an atomic spray that produces a thin film. The advantages of this technique are speed, flexibility in the choice of material, greater control of growth in any environment and an essentially clean process [15]. The composition of the target used and of the prepared thin films are quite close [16]. Many factors such as background pressure, pulse length, laser light fluency and substrate surface temperature affects the quality of the thin film deposited. Moreover, its optical properties might be tuned via a fundamental doping process [17].

In the present work, pure CdO thin films and CdO doped with CuO with different ratios in the range (0.0, 0.2, 0.3, 0.4 and 0.5) were deposited using pulsed laser deposition technique. The aim of this research is to investigate the impact of copper oxide ratio on the surface, structural, optical and electrical properties of the prepared thin films. Optical properties related to thin films might be tuned via a fundamental doping process and majorly transition metals were utilized for such purpose [18].

* Corresponding author: sundus.abbas@sc.uobaghdad.edu.iq
<https://doi.org/10.15251/JOR.2022.184.579>

2. Experiment details

Pure cadmium oxide thin films and doped with copper oxide at different ratios ($x=0.2, 0.3, 0.4$ and 0.5) were synthesized by mixing both oxide and were pressed in shapes of pellets. The pellets were subjected to a temperature of 873°K for one hour. An overall of 5 pellets were prepared: 1 pellet of pure CdO and 4 pellets of CuO doped CdO ($x = 0.2, 0.3, 0.4,$ and 0.5). Thin films from $(\text{CdO})_x (\text{CuO})_{1-x}$ targets were deposited using Nd: YAG laser of second harmonic operated with frequency of $\lambda=1064\text{ nm}$ with pulse duration of 10 ns , energy of 800 mJ and 400 pulses. The deposition was achieved in vacuum of 10^{-3} Torr . The thin films substrates were glass which was subjected to several cleaning stages to remove impurities. This was done using distilled water, alcohol and ultra-sonic bath for 15 minutes. The substrates were dried by blowing air and then a soft tissue is used for wiping. The thickness of the films was measured with an optical Michelson interferometer. The thickness of the pure films was (23nm) while that for the doped films with the different concentrations of CuO were $(39, 55, 76,$ and $100\text{ nm})$. XRD patterns were recorded with Philips PW 1050 X-ray diffractometer with Cu $K\alpha$ radiation ($\lambda = 1.5406\text{ \AA}$), 40 kV accelerating voltage and 30 mA emission current. It was utilized for analyzing the samples' crystal structures, while the films' crystallite level was specified by the crystallite size and lattice constant. The surface morphological features of the various films are examined utilizing AFM SPM-AA3000. The absorbance and transmittance spectra were measured as function of wavelength with a double beam UV-Vis-NIR Spectrophotometer in the wavelength range $200 - 1100\text{ nm}$. The electrical properties are evaluated using a four-point probe apparatus and Hall Effect technique to find out mobility, carrier density, and the type of conduction for all thin films.

3. Results and Discussions

3.1. Structural Properties of $\text{CdO}_x\text{CuO}_{1-x}$ Thin Films

Fig. 1 shows the diffraction pattern of undoped and doped cadmium oxide with different copper oxide ratios. The figure shows many peaks located at 2θ equal to $32.8, 47, 38.12, 55, 67$ degree corresponding to the planes $(1\ 1\ 1), (2\ 0\ 0), (2\ 2\ 0)$ and $(3\ 1\ 1)$ respectively. This refers to polycrystalline cubic structure which is compatible with standard card number $(96-101-1097)$. From the same figure, it is obvious that doping with copper oxide resulted in increase of FWHM causing the reduction of the peaks intensity of the prepared thin films, as shown in Table 1. On the other hand, the introduction of copper oxide to cadmium oxide led to lowering the intensity of the main plane of crystal growth $(2\ 0\ 0)$ on the expense of growing the intensity of the $(1\ 1\ 1)$ plane. This result is similar to the findings of other workers [18, 19 and 20]. It is clearly observed that increasing the copper oxide content resulted in decreasing the degree of crystallinity as well as the disappearance and of some diffraction peaks and the appearance of a new peak located at $2\theta = 24.349^\circ$ corresponding to the plane $(0\ 2\ 1)$ which is compatible with monoclinic phase copper oxide according to the standards card number $05-661$ [21]. This peak affirms the introduction of copper oxide within the cadmium oxide films. The change of crystal growth plane was found to be related to the vacancies of oxygen also may be due to the substitution of the cadmium atoms by copper atoms as the doping ratio increases [22]. It could also be related to internal stress induced by copper oxide doping to the host material, which may alter the energetic balance between various crystal planes orientations resulting in the desired texture growth. These results are in agreement with the results of Zheng et al. [19]. The addition of copper oxide in cadmium oxide may be altering the rate of diffusion and consequently changing the direction of crystal growth [23, 24].

Table 1. Structural parameters and crystallite size of CdO films for different CuO concentration.

Sample X	2Theta (Deg.)	FWHM (Deg.)	d _{Exp.} (Å)	d _{Std.} (Å)	a _{Exp.} (Å)	D (nm)	Strain 10 ⁻⁴	δ 10 ¹⁴ (lines/m ²)	hkl
0.0	32.806	0.2833	2.7278	2.7280	4.7246	30.5	11.853	10.75	111
0.2	32.847	0.3102	2.7245	2.7280	4.7189	26.7	12.976	14.03	111
0.3	32.847	0.420	2.7245	2.7280	4.7189	19.7	17.569	25.76	111
0.4	32.907	0.7140	2.7196	2.7280	4.694	11.6	29.863	74.32	111
0.5	24.349	0.3890	3.6526	3.6514		16.9	16.583	35.01	021

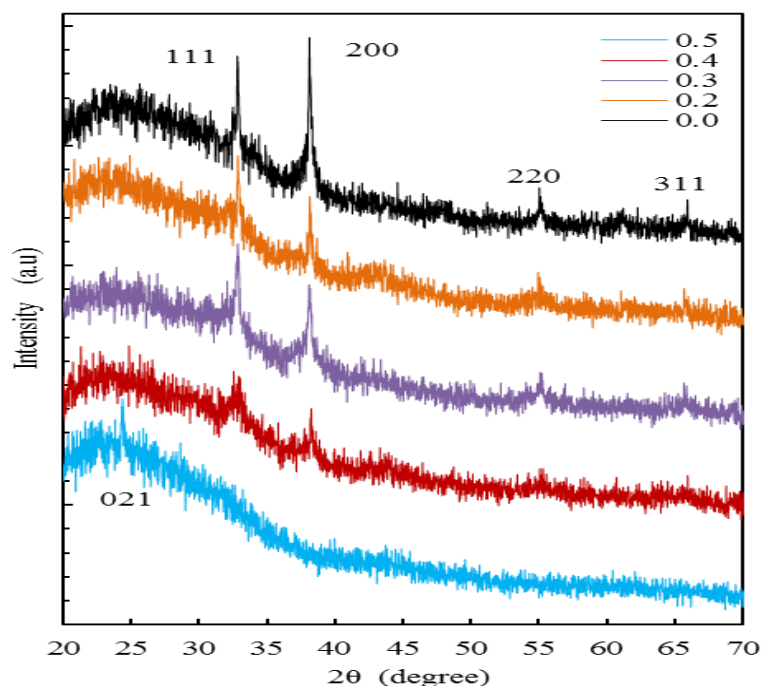


Fig. 1. XRD patterns of pure CdO and $(\text{CdO})_x(\text{CuO})_{1-x}$ thin films.

The crystallite size was estimated using Debye-Scherrer's formula [25, 26]:

$$D = 0.94\lambda / \beta \cos \theta \quad (1)$$

where λ is the wavelength of x-ray (1.54060Å), and β represents full-width at half maximum (FWHM).

The addition of copper oxide may result in more defects giving rise to large deformation of lattice structure [27]. From Table 1, it is clear that the location of diffraction peaks has shifted towards higher angles values by the addition of copper oxide. This occurred as a result of shrinkage of the lattice parameter since copper atoms are located at grain boundaries or at the surface, whereas there is a minor reduction in the value of d-spacing at high copper content ($x > 0.3$). The more pronounced effects of Cu^{+2} ions infer that Cu^{+2} ions replace Cd^{+2} ions in host lattice substitutionally. The slight changes of lattice constants might be due to the substitution of the rather large Cd^{+2} ions of radius 0.96 Å by the smaller Cu^{+2} ions of radius 0.73 Å ions. This causes the shrinking of CdO crystal lattice, which reduces the crystallite size. This result is similar to that reported by Aydogu et al. [23] and Usharani et al. [24].

From Fig. 2, it is obvious that doping with copper oxide resulted in increase of FWHM giving rise to reduction of the crystallite size of the prepared thin films. Such a reduction in the

peak intensity with CuO doping might be due to producing further lattice defects and lattice strains in films [17].

The dislocation density (δ) was calculated using the following relation [28, 26]:

$$\delta = 1/D^2 \quad (2)$$

The dislocation density increased by increasing copper content in the prepared thin films (see Table 1); the growing of dislocation density proposes that the addition of copper oxide has induced defects in thin films which resulted in hindering the growth of the crystal. The dislocations are of high importance concerning surface properties [8].

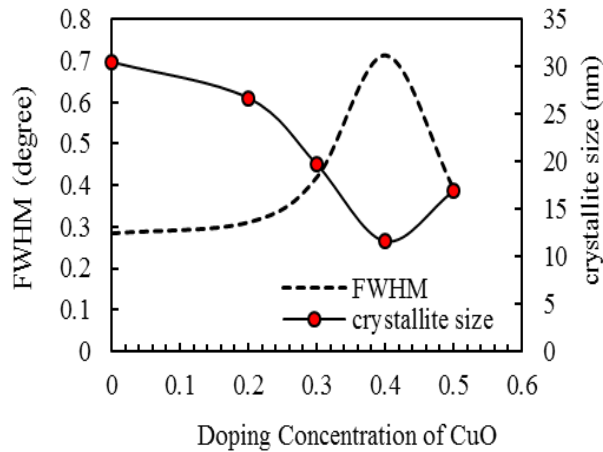


Fig. 2. Variation in the FWHM and crystallite size of $(CdO)_x(CuO)_{1-x}$ thin films.

Strain (ϵ) was calculated using the following relation [26]:

$$\epsilon = \beta \cos \theta / 4 \quad (3)$$

The reduction in crystallite size with the increase of copper content occurred as a result of the high strain. Table 1 indicates that there was an increase in the strain for the films with the reduction of crystallite size. This might be because of the CuO accumulation on grain boundaries regarding CdO which inhibits the crystal growth and results in strain generated in the CdO grains [29]. Figure 3 shows the dislocation and strain as a function of copper content in thin films.

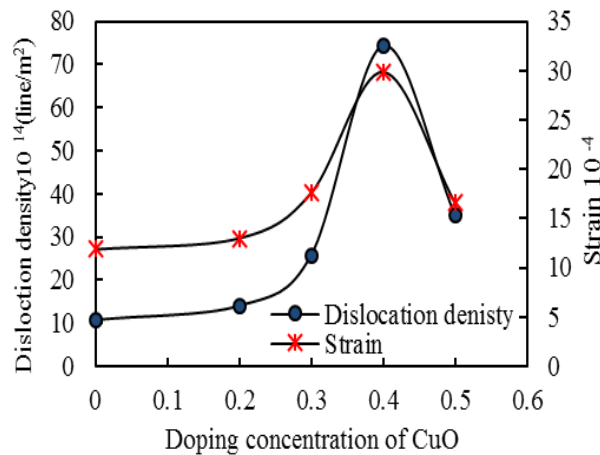


Fig. 3. Variation in the dislocation density and strain of $(CdO)_x(CuO)_{1-x}$ thin films.

3.2. Atomic Force Microscope (AFM)

AFM measurements enable the determination of the effect of preparation conditions such as thickness, deposition temperature, compositions, on the synthesized samples [29]. Figure 4 illustrates two-dimensional (2D) and three-dimension (3D) images of the AFM of pure CdO and $(\text{CdO})_x(\text{CuO})_{1-x}$ thin films with different copper oxide content. The AFM images of pure CdO thin films show uniform surface morphology that has numerous voids while the surface of thin films with low copper oxide $x=0.2$ seems rough in comparison with the pure CdO thin films, this is in agreement with Gültekin et al. [30].

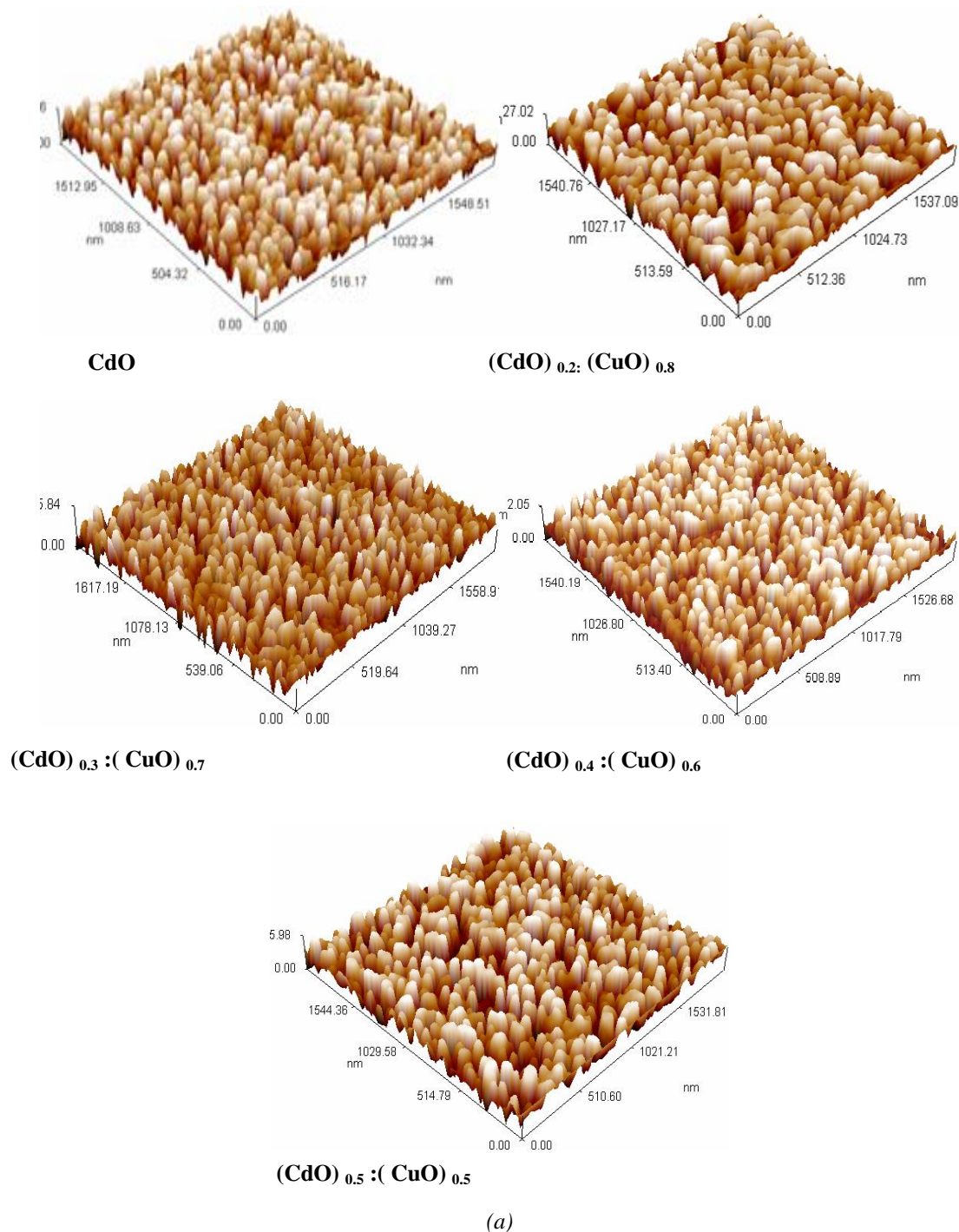


Fig. 4.1 AFM images of pure CdO and $(\text{CdO})_x(\text{CuO})_{1-x}$ thin films (a) the three-dimensional

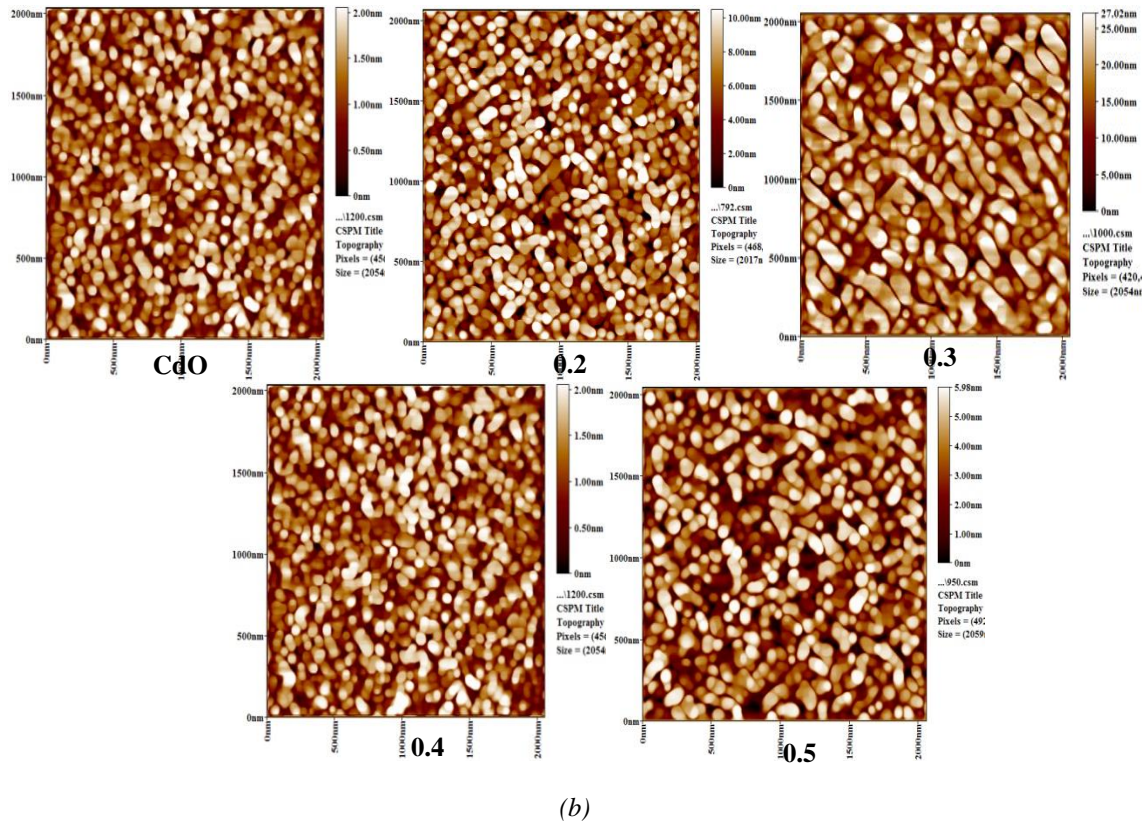


Fig. 4.2 AFM images of pure CdO and $(\text{CdO})_x(\text{CuO})_{1-x}$ thin films (b) two-dimensional.

The results showed that both the average diameter and roughness have increased by the introduction of copper oxide to the host materials, indeed the average diameter of 63.83 nm and surface roughness of 2.63 nm were increased to 68.46 nm and 6.23 nm, respectively when x increased from 0 to 0.2. The results in Table 2 shows that both the roughness and average diameter is changing in a non-regular manner (i.e. decreasing and increasing) with the increase of copper oxide content. The reduction of roughness and average diameter by the increase of copper oxide is ascribed to the intrinsic stress due to introduction of foreign atoms, thus the addition of CuO led to formation of thin films with high smoothness or thin films with organized distribution of CuO, this is similar to previous reported results [4, 11 and 31]. The reduction of films roughness results in the reduction of scattering of incident light which consequently increases the optical transmittance [32].

Table 2. Average roughness R_a , average diameter and RMS of CdO films with CuO doping.

Sample X	R_a (nm)	RMS (nm)	Grain size XRD (nm)	Avg. Diameter AFM (nm)
0	2.19	2.63	28.0	63.83
0.2	5.24	6.23	26.7	68.46
0.3	1.09	1.31	19.7	62.11
0.4	0.42	0.49	11.6	74.69
0.5	1.35	1.59	16.9	67.46

3.3. Optical analysis

Figure 5 illustrates transmittance as function of wavelength for undoped and doped CdO thin films. It is seen that the transmittance increases with increasing the wavelength. The results

showed that the value of transmittance of undoped CdO film was around 24% to 45% in the visible region while the transmittance grow up when copper oxide was added to reach 76% in the visible area. The transmittance reached maximum value of 85% at $x= 0.4$. But, it was reduced drastically at $x= 0.5$. These results indicate that the addition of copper oxide improves the transmittance of the host material to be in the range 52% and 85%. This resulted from the significant reduction of absorption when copper oxide was added to cadmium oxide. The structural modification such as impurity and defects, which causes a reduction of crystal size (as seen from x-ray diffraction patterns) as copper oxide is added to cadmium oxide is responsible for the high transmittance and low absorbance. Similar results were obtained by other workers [33, 34 and 35]. The high transmittance values of $(\text{CdO})_x(\text{CuO})_{1-x}$ thin films refereed that the prepared samples are most convenient for solar cell applications as a window layer. The obtained data declared that the transmittance was 85% at $x= 0.4$ while it was reduced drastically at $x=0.5$. This occurred because of the metallic nature of the prepared thin films, which leads to high absorption or low transmissions. Absorption coefficient α was computed from the Beer Lambert law [36]. Figure 6 shows the relation between the absorption coefficient and wavelength. Tauc's relation was used to determine the optical energy gap of $(\text{CdO})_x(\text{CuO})_{1-x}$ thin films [37]:

$$(\alpha h\nu)^2 = A(h\nu - E_g) \quad (4)$$

where A , α , n , E_g , ν and h are a constant, the absorption coefficient, a constant that depends on the type of optical transition (1/2, 2 for the direct and indirect allowed transition and 3/2, 3 for the direct and indirect forbidden transition), the optical band gap, the frequency and plank constant respectively. Figure 7 shows the relation between energy and $(\alpha h\nu)^2$ of pure and CuO doped CdO thin films. This affirms direct allowed transition ($n=1/2$) as pointed out by many researches [38, 39]. The energy gap values were determined from the intercept of the straight line of the plots with the energy axis. The values of optical energy gap were listed in Table 3. It is noticed that E_g for cadmium oxide was 2.4 eV. The values of E_g increased by increasing the copper oxide content in the prepared thin films. It has increased from 2.4 to 3.51 eV when copper oxide content increased from 0 to 0.5. The optical energy gaps values exceeded the values of published values of CuO doped CdO films using PLD Menazea et al. [18] reported a value of (3.39 eV) while that reported by Rahman et al. was (2.90 eV) [40]. The blue shift of the energy gap was related to low crystallinity as a result of more disorder accompanied with the increase of CuO doping [41]. This blue shift may be explained according to the Burstein-Moss (BM) effects [42, 43] which take place when drastic increase of carrier concentration happens [44].

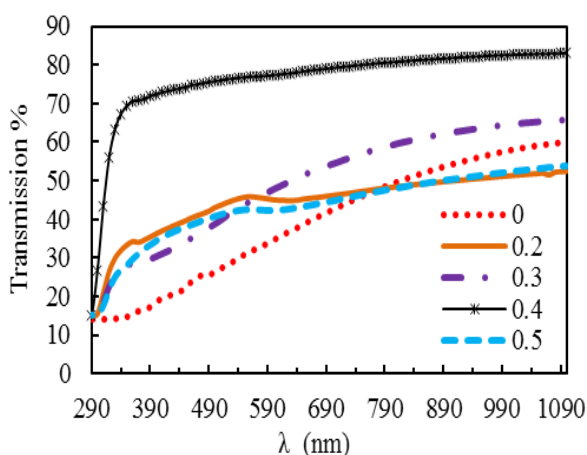


Fig. 5. Transmittance spectra of $(\text{CdO})_x(\text{CuO})_{1-x}$ thin films.

The pronounced reduction of absorption at high copper oxide content can be ascribed to reduction of crystallite size which causes the blue shift of energy gap. This was confirmed by x-ray diffraction results. It is well; known that the addition of CuO may result in increase or decrease of the number of electrons in conduction bands which causes shifting of Fermi level accompanied by changes in the energy gap. This widening has been significant for the applications of the TCO, like the applications in optoelectronic industries, especially for the applications of the solar cells.

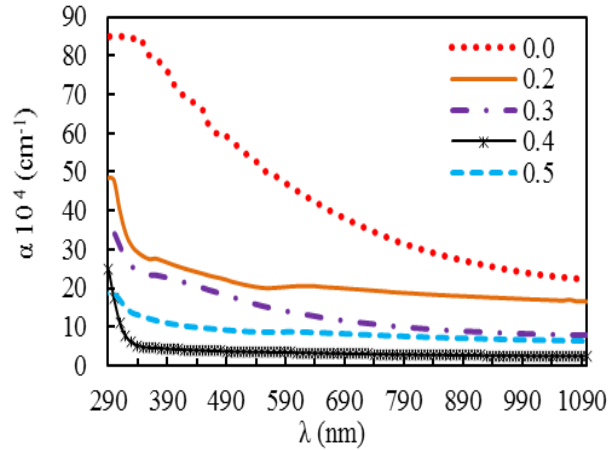


Fig. 6. Variation of absorption coefficient as a function of wavelength.

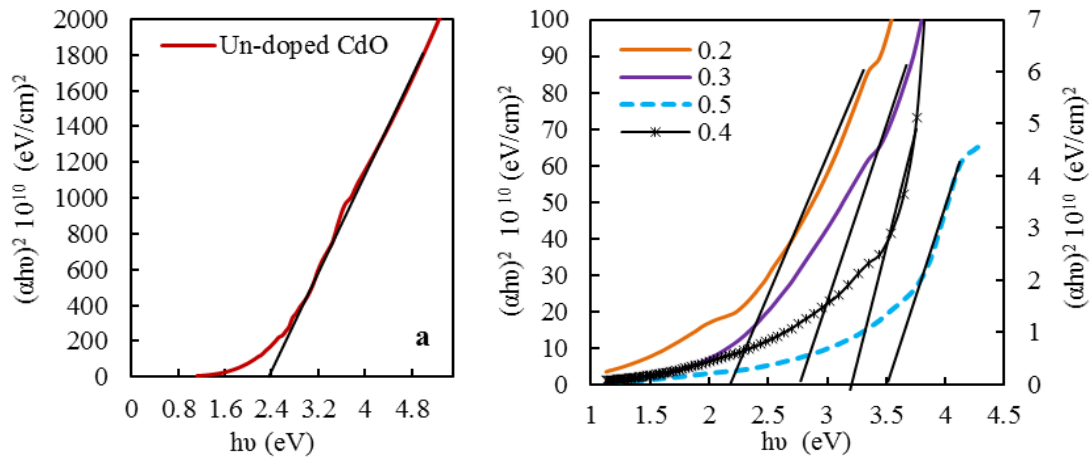


Fig. 7. Plots of $(\alpha h\nu)^2$ versus $(h\nu)$ for (a) un-doped CdO and (b) CuO doped CdO thin films.

Table 3. The calculated values of energy band gap of CdO films with different CuO content.

CdO concentration	E_g (eV)
0.0	2.4
0.2	2.25
0.3	2.75
0.4	3.3
0.5	3.51

3.4. Electrical properties

Hall measurements were conducted in order to obtain the electrical characteristics of $(\text{CdO})_x (\text{CuO})_{1-x}$ thin films such as the type of conductance, mobility and carrier concentration. Hall measurements revealed the fact that the pure CdO and $(\text{CdO})_x (\text{CuO})_{1-x}$ thin films are n-type when x value was in the range (0 to 0.4) but further addition of CuO converted the samples to p-type. The of carrier concentration, resistivity, conductivity, and mobility with changing the CuO content are listed in Table 4. It can be observed that the electrical parameters are highly affected by the CuO content in the prepared thin films. The effects of the copper oxide content on the carrier density are illustrated in Figure 8. From Table 3, it is seen that pure films show higher carrier concentration of $2.132 \times 10^{23} \text{ cm}^{-3}$ which was reduced to $3.7 \times 10^{11} \text{ cm}^{-3}$ when copper content was $x=0.5$. The carrier density of the CdO film decreased with the increase in the CuO content. This proposed that the copper oxide atoms will be not ionized readily and some of those play the role of CdO thin films' neutral impurities. This was mentioned by Kumaravel et al. and Ahmed et al. [4, 49]. Simultaneously, the CdO film carrier mobility increased with increasing CuO content and reached a maximum value of $199.5 \text{ cm}^2/\text{V.s}$ when copper content was $x=0.5$. The increase of carrier mobility is ascribed to lower potential barrier height of the grain boundaries which enable the charge carriers to travel easily over the boundaries of the grain, this will increase the carrier mobility. Similar behavior has been observed by [45, 46].

From Figure 9, it is clearly observed that the electrical resistivity of $(\text{CdO})_x (\text{CuO})_{1-x}$ films increased with the increase in CuO content. It can be noticed as well, that initially, resistivity increased slowly with CuO content, and then rapidly to reach a maximum value of $8.25 \times 10^4 \text{ } \Omega \text{ cm}$. This increase in the resistivity with the CuO content is attributed to the decrease in grain size resulting in the increase scattering at the grain boundary which will result in the decrease of conductivity. The high resistivity value that occurred at $x > 0.3$ suggested that many disorder sites have been created in lattice as a result of the ions of the Cu^{2+} as mentioned in x-ray diffraction. The ions of the Cu^{2+} act as recombination centers. In addition to that the formation of neutral defects at high CuO content with the reduction of grain size resulted in the growing of the resistivity, this matched the results of AFM analyses.

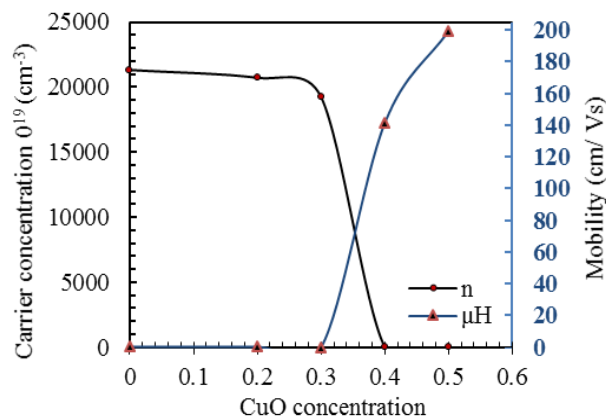


Fig. 8. Carrier concentration (n) and mobility (μ_H) of the $(\text{CdO})_x (\text{CuO})_{1-x}$ thin films as a function of CuO content.

Table 4. The calculated values of conductivity, resistivity, carrier concentration, Hall mobility of $(\text{CdO})_x (\text{CuO})_{1-x}$ thin films

Sample X	σ ($\Omega \cdot \text{cm}$) ⁻¹	ρ 10 ⁻⁴ $\Omega \cdot \text{cm}$	μ_H $\text{cm}^2/\text{V} \cdot \text{s}$	n_H (cm^{-3})	Type of conductivity
0.0	2.934×10^3	3.419	0.25664	2.132×10^{23}	n-type
0.2	2.563×10^3	3.902	0.26435	2.071×10^{23}	n-type
0.3	5.702×10^2	17.54	0.07014	1.923×10^{23}	n-type
0.4	1.247×10^2	81.49	141.5	1.120×10^{19}	n-type
0.5	1.138×10^{-5}	$8251 \times 10^{+4}$	199.5	3.703×10^{11}	p-type

The conductivity of the prepared $(\text{CdO})_x (\text{CuO})_{1-x}$ thin films changed in reverse manner to resistivity, i.e. higher conductivity was obtained for pure CdO ($2.934 \times 10^3 \Omega^{-1} \text{cm}^{-1}$) and decreased to the minimum value of $1.138 \times 10^{-5} \Omega^{-1} \text{cm}^{-1}$ by increasing the CuO content. The particle size reduction results in the increase of the boundary volume of the grain within deposited films, increasing the scattering of the grain boundary for moving charge carriers. In addition, increasing the CuO content will increase the strain and the dislocation density as mentioned previously, which introduces more defects related with cadmium interstitials and oxygen vacancies which resulted in an increase of the resistance of the $(\text{CdO})_x (\text{CuO})_{1-x}$ films. Similar results were obtained by Ghosh et al. [47]. The change of the conductance type from n- to p-type may come from the co-existence of the CuO doped CdO phases as well as from the impurity of the copper oxide.

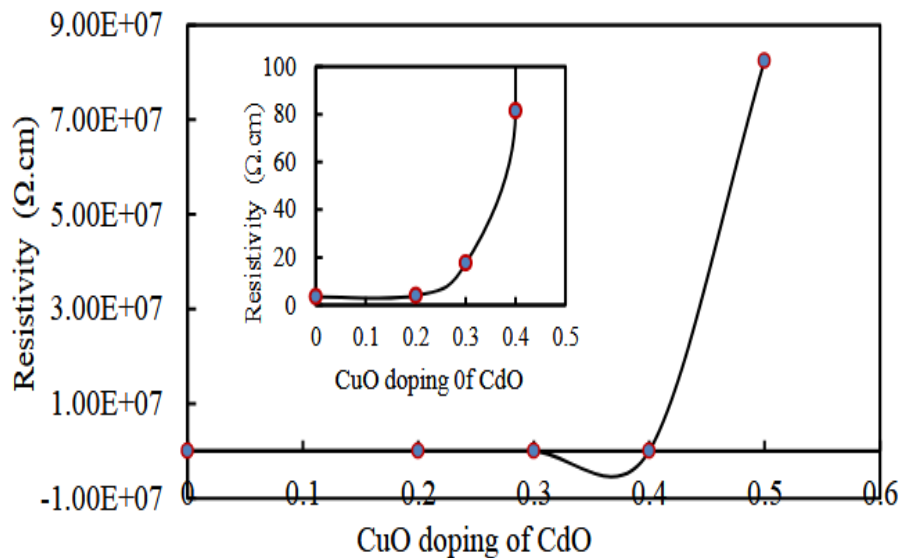


Fig. 9. The resistivity (ρ) of the $(\text{CdO})_x (\text{CuO})_{1-x}$ films thin films as a function of CuO content, the inset shows the variation in resistivity variation with CuO at low concentrations.

4. Conclusion

The impact of CuO content on the morphological, structural, optical and electrical properties of CdO thin films that have been produced by the PLD technique was examined. From X-ray diffraction, it was found that there was an increase in diffraction peaks intensity at (1 1 1) as well as a decrease in diffraction peaks intensity at (2 0 0) that confirms the doping growth of the CuO via the of the CdO film. From Atomic Force Microscopy, it was shown that there was decrease in grain size along with the increase in CuO content. Additionally, the value of the transmittance had increased with the increase in the CuO content reaching maximum value of 85% at $x = 0.4$. The results showed that the band gap value of the prepared $(\text{CdO})_x (\text{CuO})_{1-x}$ thin films increased from 2.4 to 3.51 eV by increasing CuO content from 0 to 0.5. Also, the results showed that the carrier concentration decreased with increasing CuO content and reached a minimum value of $3.703 \times 10^{11} \text{cm}^{-3}$ when CuO content was 0.5, resulting in electrical resistivity incensement.

References

- [1] H. Ullah, R. Rahaman and S. Mahmud, Indonesian J. Elec. Eng. Comp. sci. 5 (1), 81 (2017); <https://doi.org/10.11591/ijeecs.v5.i1.pp81-84>

- [2] B. Şahin, *Physical Scientific World Journal* 3, 1 (2013).
- [3] R. Zargar, S. Chackrabarti, M. Arora and A. Hafiz, *Int. Nano. Lett.* 6 (2), 99 (2016); <https://doi.org/10.1007/s40089-015-0172-5>
- [4] R. Kumaravel, S. Menaka, S. Regina, M. Snega, K. Rama- murth and K. Jeganthn, *Mater. Chem. Phys.* 122 (2-3), 444 (2010); <https://doi.org/10.1016/j.matchemphys.2010.03.022>
- [5] G. Shanmugaval, A. Balu and V. Nagarethnam, *Int. J. Chem. Mater. Res.* 2 (9), 88 (2014).
- [6] G. Naser, W.N. Raja, A.S. Faris, J.Z. Rahemd, M.A. Salih and A.H. Ahmed, *Energy Procedia* 36, 42 (2013); <https://doi.org/10.1016/j.egypro.2013.07.006>
- [7] A. K. Elttayef, H.M. Ajeel and A.I. Khudiar, *J. Mater. Res. Technol.* 2 (2), 182 (2013); <https://doi.org/10.1016/j.jmrt.2013.02.004>
- [8] M. Ghosh and C.N.R. Rao, *Chem. Phys. Lett.* 393 (4-6), 493 (2004); <https://doi.org/10.1016/j.cplett.2004.06.092>
- [9] A. U. Ubale, S.S. Wadnerkar, P. Sononeand and G. Tayde, *Arch. Phys. Res.* 5 (6), 43 (20-14).
- [10] K. Siraj, M. Khaleeq-ur-Rahman, S. I. Hussain, M. S. Rafique and S. Anjum, *Journal of Alloys and Compounds* 509 (24), 6756 (2011); <https://doi.org/10.1016/j.jallcom.2011.03.183>
- [11] O. Ali, *J. Appl. Phys.* 9 (1), 1 (2017).
- [12] S. M. Mahdavi, A. Irajizad, A. Azarian and R. M. Tilaki, *Scientia Iranica*, 15 (3), 360 (2008).
- [13] A. H. Alkhayatt, I.A. Al-hussainy and O. Al-rikaby, *Adv. Phys. Theor. Appl.* 34 (1), 1 (2014).
- [14] A. A. Yousif and M. H. Hasan, *Iraqi J. Appl. Phys.* 11 (1), 15 (2015).
- [15] N. H. Harb, *Baghdad Sci. J.* 15 (3), 300 (2018); <https://doi.org/10.21123/bsj.15.3.300-303>
- [16] M.A. Saliyam, I.M. Ibrahim and I.M. Ali, *Indian J. Natural, Sci.* 9 (5), 15384 (2018).
- [17] I. Ali, Z. Ullah, K. Siraj, M.S. Rafique and M.K. ur-Rahman, *Int. J. Thin Film Sci. Tech.* 3 (3), 107 (2014); <https://doi.org/10.12785/ijfst/030305>
- [18] A.A. Menazea, A.M. Mostafa and E.A. Al-Ashkar, *Opt. Mater.* 100 (4), 109663 (2020); <https://doi.org/10.1016/j.optmat.2020.109663>
- [19] B.J. Zheng, J.S. Lian, L. Zhao and Q Jiang, *Vacuum* 85 (9), 861 (2011); <https://doi.org/10.1016/j.vacuum.2011.01.002>
- [20] R. Kumaravel, K. Ramamurthi and V. Krishnakumar, *J. Phys. Chem. Solids* 71 (11), 1545 (2010); <https://doi.org/10.1016/j.jpcs.2010.07.021>
- [21] C. Tamuly, I. Saikia, M. Hazarika and M. Das, *Roy. Soc. Chem. Adv.* 4 (95), 53229. (2014); <https://doi.org/10.1039/C4RA10397A>
- [22] A. Kathalingam, K. Kesavan, A. H. Rana, J. Jeon and H. Kim, *Coatings* 8 (5), 167 (2018); <https://doi.org/10.3390/coatings8050167>
- [23] S. Aydogu, G. Çabuk, M. B. Çoban, *J. Natural Appl. Sci.* 23 (1), 140 (2019).
- [24] K. Usharani, A. Balun, V. Nagarethiam and M. Suganya, *Prog. Nat. Sci.: Mater. Int.* 25 (3), 251 (2015); <https://doi.org/10.1016/j.pnsc.2015.06.003>
- [25] B.D. Cullity "Elements of X-ray Diffraction" Addison-Wesley, Massachusetts, p. 99 (1956).
- [26] N. Ali, N. Hussein, B. Chiad and S.M. Al-dujayli, *Indian J. Pure Appl. Phy.* 56 (1), 13 (2018).
- [27] M. Sajjad, I. Ullah, M.I. Khan, J. Khan, M.Y. Khan and M.T. Qureshi, *Res. Phys.* 9 (9), 1301 (2018); <https://doi.org/10.1016/j.rinp.2018.04.010>
- [28] G.K. Williamson and R. Smallman, *philos. Mag.* 1 (1), 34 (1956); <https://doi.org/10.1080/14786435608238074>
- [29] N.B. Hasan and M.J. Mohammed, *Inter. Lett. Chem. Phys. Astro.* 58, 102 (2015).
- [30] A. Gültekin, G. Karanfil, F. Özel, M. Kuş, R. Say and S. Sönmezoğlu, *Eur. Phys. J. Appl. Phys.* 64 (3), 30303 (2013); <https://doi.org/10.1051/epjap/2013130418>
- [31] G. Singh, S.B. Shrivastav, D. Jain, S. Pandya, T. Shripathi and V. Ganesan, *Bull. Mater. Sci.* 33 (5), 581 (2010); <https://doi.org/10.1007/s12034-010-0089-6>
- [32] M. Thirumoorthi and J. Prakash, *J. Asian Ceram. Soc.* 4 (1), 124 (2016); <https://doi.org/10.1016/j.jascer.2016.01.001>
- [33] M. Yüksel, B. Şahin and F. Bayansal, *Ceram. Int.* 42 (5), (2016) 6010;

<https://doi.org/10.1016/j.ceramint.2015.12.154>

- [34] Z. Zhao, D. Morel and C.S. Ferekides, *Thin Solid Films* 413 (1-2), 203 (2002);
[https://doi.org/10.1016/S0040-6090\(02\)00344-9](https://doi.org/10.1016/S0040-6090(02)00344-9)
- [35] J.A. Abd, R.T. Ahmed and N.A. Mohamed, *Australian J. Basic Appl. Sci.* 8 (Special 3), 166 (2014).
- [36] F. Ables "Optical Properties of Solids" Amsterdam: North Holland, New York, p. 32 (1972).
- [37] J. Tauc, *Mater. Res. Bull.* 5 (8), 721 (1970); [https://doi.org/10.1016/0025-5408\(70\)90112-1](https://doi.org/10.1016/0025-5408(70)90112-1)
- [38] S. Aksoy, Y. Caglar, S. Ilican, M. Cağlar, *Int. J. Hydrogen. Energy* 34 (12), 5191 (2009);
<https://doi.org/10.1016/j.ijhydene.2008.09.057>
- [39] A.M. Darwish, W.H. Eisa, A. Shabaka and M.H. Talaat, *pectrochimica Acta Part A: Molecular and Biomolecular Spectroscopy* 153 (2), 315 (2016);
<https://doi.org/10.1016/j.saa.2015.08.007>
- [40] M. Rahman, M. Hussain and A. Asiri, *Prog. Nat. Sci.: Mater. Inter.* 27 (5), 566 (2017);
<https://doi.org/10.1016/j.pnsc.2017.08.014>
- [41] S. Tewari and A. Bhattacharjee, *Pramana- J. Phys.* 76 (1), 153 (2011);
<https://doi.org/10.1007/s12043-011-0021-7>
- [42] T. S. Moss, *Proc. Phys. Soc. Ser. B* 67 (10), 775 (1954); <https://doi.org/10.1088/0370-1301/67/10/306>
- [43] A. Dakhel and A. Ali Mohamed, *J. Sol. Gel. Sci. Technol.* 44 (3), 241 (2007);
<https://doi.org/10.1007/s10971-007-1615-x>
- [44] N.E. Makori, I.A. Amatal, P.M. Karmi and W.K. Njoroge, *Inter. J. Optoelect. Engin.* 4 (1), 11 (2014).
- [45] S. Ahmed, M.S. Sarker, M.M. Rahman, M. Kamruzzaman, M. Khan, *Heliyon*, 4 (8), 1 (2018); <https://doi.org/10.1016/j.heliyon.2018.e00740>
- [46] M. Yan, M. Lane, C.R. Kannewurf, R.P. Chang, *Appl. Phys. Lett.* 78 (16), 2342 (2001);
<https://doi.org/10.1063/1.1365410>
- [47] A. Ghosh, N. Kumari and A. Bhattacharjee, *Pramana- J. Phys.* 84 (4), 621 (2015);
<https://doi.org/10.1007/s12043-014-0851-1>